NPIC ROUTING SLIP

FROM: DATE:

	TO	INITIALS	DATE	REMARKS
DIR				
DEP/DIR				
EXEC/DIR				
ASST FOR ADMIN				
ASST FOR OPS				
ASST FOR PA				
ASST FOR P&D				
CH/CSD				
CH/PD				
CH/PSD				
CH/TID				
CH/CIA/PID				
CH/DIA/NPIC				
CH/SPAD				
LO/NSA				

STAT

STAT

MEMORANDUM FOR:

(DATE)

REPLACES FORM 10-101

INFRARED SURVEYS OF HAWAIIAN VOLCANOES

by

W. A. Fischer and R. M. Moxham—U.S. Geological Survey
F. Polcyn—University of Michigan
G. H. Landis—Aero Service Corporation

Reprinted from Science, November 6, 1964, Vol. 146, No. 3645, pages 733-742

Infrared Surveys of Hawaiian Volcanoes

Aerial surveys with infrared imaging radiometer depict volcanic thermal patterns and structural features.

W. A. Fischer, R. M. Moxham, F. Polcyn, G. H. Landis

Kilauea, on the island of Hawaii, has been one of the most active volcanoes in historic time. Though it has been studied intensively since establishment of the Hawaiian Volcano Observatory in 1912, little is known of the thermal regime, despite its obvious importance in volcanic processes. Published data include those of Jaggar (*1*), Ault and his co-workers (*2*), and Macdonald (*3*).

Obvious surficial thermal anomalies are associated with Kilauea, as visible steaming in many places attests to convective transfer of heat from subterranean sources. Ground adjacent to these steaming cracks commonly is abnormally warm. But the relative intensity and spatial configuration of the thermal patterns of this extensive volcanic system cannot easily be recorded by conventional means.

Modern infrared imaging radiometers have enabled us to map the distribution of anomalies associated with Kilauea and Mauna Loa, including some that have later been sites of volcanic eruption. These instruments have also made it possible to locate fresh water springs discharging into the ocean and to demonstrate relationships between surface configuration and consolidation and infrared emission that warrant further study, because of their possible application to lunar and planetary investigations.

Infrared radiometers have been used for many years to make surface-temperature (or, more strictly, energy-emission) measurements, but their application has generally been limited to spot measurements or traverses. In the last decade, airborne electromechanical imaging infrared radiometers have been developed for military purposes (*4*). We feel that these instruments could be adapted to thermal mapping for geophysical purposes. Instruments of this type, as they evolve, will doubtless provide quantitative data, but the present instrument configuration has provided only qualitative results. In this preliminary account we describe the data obtained for surface temperatures of Hawaii through the use of such a scanning device, supplemented by conventional aerial infrared and black-and-white photography. These sensors covered the 0.4- to 14-μ region of the electromagnetic spectrum, providing, in pictorial form, a measure of the electromagnetic energy being emitted or reflected from the earth's surface in that spectral region. The earth radiates energy whose spectrum approximates that of a black body at 300°K (Fig. 1), with a maximum near 9.5 μ. In addition, during daylight hours the earth reflects solar energy whose spectrum approximates that of a black body at 6000°K, with a maximum near 0.5 μ. The energy emitted or reflected from the earth's surface is selectively absorbed by the atmosphere, so only that part which passes through atmospheric windows (Fig. 2) reaches an airborne detector.

The sensors were carried in an A-26B aircraft operated by Aero Service Corporation. That organization was also responsible for the photography. Infrared imaging was carried out by the University of Michigan's Institute of Science and Technology. The aerial surveys were made from 26 January to 20 February 1963, under the direction of the U.S. Geological Survey.

W. A. Fischer and R. M. Moxham are affiliated with the U.S. Geological Survey, Washington, D.C.; F. Polcyn is on the staff of the Infrared Radiation Laboratories, Institute of Science and Technology, University of Michigan; G. H. Landis is affiliated with the Aero Service Corporation, Philadelphia, Pa., a division of Litton Industries.

Geologic Setting

Kilauea is a shield volcano built against the east side of its larger neighbor, Mauna Loa (Fig. 3). The volcano has grown to an altitude of about 1200 meters from repeated outpourings of basaltic lava along two major rift zones. At the summit is a caldera about 4 kilometers in diameter, whose floor is formed of lava erupted in historic time, most recently in 1954. Steam issues from arcuate patterns of cracks on the caldera floor and from several other localities adjacent to the caldera. Some cracks yield pure water vapor; some yield steam, at near-normal steam temperature, carrying salts in solution (for example, Sulfur Banks). A few, as at the crest of the Kilauea Iki cinder cone, are superheated. Halemaumau, a crater in the southwest part of the caldera, has been the scene of repeated volcanic activity. For many years it was filled with liquid lava, but the crust is now solidified. Adjacent to the caldera on the east is Kilauea Iki, a crater filled by a lava lake during a spectacular eruption in 1959 (*5*).

Two major rift zones transect the volcano. The east rift zone of Kilauea is a curvilinear system of faults, extending southeast from the summit area, thence east and northeast, where it intersects the coastline at Cape Kumukahi. Near the summit the rift is marked by a chain of pit craters; toward the east, open fissures and cinder cones are more common. The other major rift zone curves southwest from the summit to the sea. It is thought that, in the eruptive cycle of Kilauea, lava enters the summit area through a system of conduits beneath Halemaumau and commonly is discharged through tubes that follow the two rift zones. In the past two decades most of the lava eruptions have been in Halemaumau or along the east rift zone. The latest eruption prior to the survey discussed here was on 7 December 1962, when about 335,000 cubic meters of lava were discharged into and near Aloi Crater. (For additional details on the geology of Kilauea, see *6* and *7*.)

Instrumentation

The following aerial sensors were used.

1) An infrared scanner (Fig. 4) that records an image whose gray scale is controlled by the instantaneous energy focused upon the detector. Detecting elements sensitive to radiation in the 2- to 6-μ and 8- to 14-μ parts of the spectrum were used. The energy radiated from the earth's surface, and hence the image gray scale, is a function of surface temperature and emissivity. As emissivity of earth materials and vegetation ranges from perhaps 0.7 to 0.98, the image tone depicts what we term "apparent surface temperatures." Lighter shades on the accompanying images indicate higher apparent surface temperatures.

2) Infrared aerial photography (long-wavelength cutoff, $\sim$ 0.9 μ) which records reflected solar infrared energy. These photographs helped identify features that were seen on other images and provided a means of estimating relative absorption of solar energy. Darker tones indicate greater absorption.

3) Conventional aerial photography, to assist in identification and to provide information on surface configuration and absorption of solar energy.

In the following discussion the records provided by the infrared scanning technique are termed *images*; the term *photographs* is used only for records obtained by conventional aerial cameras.

Temperature Measurements on the Ground

Figure 5 shows air temperatures and surface temperatures of several objects measured with a contact pyrometer. The apparent temperature of the soil, rock outcrops, and vegetation in a small area warmed by volcanic steam varied relatively little during the hours 0200 to 1000 (all times given here are local standard time), while other nearby materials show a normal diurnal temperature curve. Thus, between 0200 and daybreak at about 0630 (and probably for several hours before 0200), thermal anomalies have maximum contrast with their natural surroundings; this finding is confirmed by the infrared images shown in Figs. 6 and 7. The basalt outcrop and the blacktop road are very faint or absent in the 0640 image, whereas at 1008 they are nearly as bright as the thermal anomalies.

Field measurements made during this study suggest that the temperatures of some thermal sources vary with time; for instance, temperature of the ground surface adjoining a small steaming vent near Aloi Crater ranged from about 29° to 41°C during the survey period. The vent is in an active collapse area resulting from the December 1962 eruption.

Minor, short-term variations in temperature are related to changes in sky temperature, relative humidity, volcanic action, and rainfall. Rainfall is thought to be particularly significant; it percolates downward through the highly permeable volcanic rocks, is heated, and subsequently vented as steam or warm vapor. Many thermal anomalies on the infrared images correlate with this visible evidence of convective heat transfer.

Classification of Thermal Sources

A thermal source of given area and emissivity, as its temperature increases, emits increasing amounts of energy at decreasingly shorter wavelengths. Three anomaly groups were established through contrast of their relative emission in different parts of the infrared spectrum. The thermal sources were further classified into seven orders of magnitude, designated by roman numerals which indicate the relative amounts of energy emitted; the higher the energy, the smaller the numeral. Magnitude assignment within groups was accomplished by densitometer measurement of relative image brightness.

Group 1 (magnitudes I, II, and III). Sources visible on all infrared images, including those recording wavelengths $< 2.6\ \mu$.

Group 2 (magnitudes IV, V, and VI). Sources which appear only on images recording wavelengths $> 2.6\ \mu$.

Group 3 (magnitude VII). Sources which appear only on images recording wavelengths $> 5.5\ \mu$.

Measurements on the ground suggest that magnitude III sources have temperatures 5° to 10°C (varying with time) above ambient temperature (apparent temperature of the surrounding area). Locally this group may include small sources having appreciably higher temperatures.

Kilauea Summit Area

The dominant volcanic and structural features of the Kilauea summit area, as depicted by various sensors, are shown in Figs. 8–11. The spectral response of the infrared detectors was controlled by interference filters; Fig.

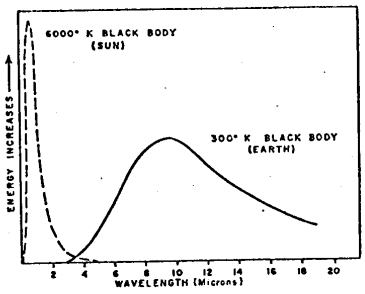

Fig. 1. Radiation curves for black bodies at temperatures of 6000° and 300°K. Earth materials, being "gray bodies," depart from this curve according to their spectral emissivity.

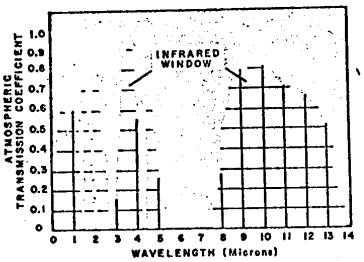

Fig. 2. Atmospheric transmission in the visible and the infrared regions of the spectrum.

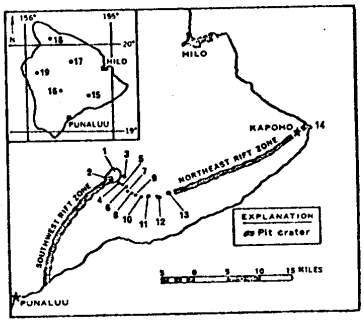

Fig. 3. Volcanic and other features of Hawaii. 1, Kilauea caldera; 2, Halemaumau; 3, Kilauea Iki; 4, Keanakakoi; 5, Lua Manu; 6, Puhimau; 7, Kokoolau; 8, Heake; 9, Pauahi; 10, Aloi; 11, Alae; 12, Makaopuhi; 13, Napau; 14, Cape Kumukahi. Inset: 15, Kilauea; 16, Mauna Loa; 17, Mauna Kea; 18, Kohala; 19, Hualalai.

10 (right) shows only the hotter areas, Fig. 10 (left) shows the smaller variations in apparent surface temperatures but does not resolve the hotter areas, and Fig. 11 is a compromise between these two extremes.

Most of the peripheral faults of the caldera show, on the infrared images, some thermal abnormality, ranging from very indistinct diffuse linear patterns to highly localized anomalies that are believed to be correlated with steaming vents. The caldera floor is reticulated, with curvilinear elements of greatly varying intensity that also correspond in part to steaming fissures. One prominent subcircular feature [*D* in Fig. 11, *a* and *b*] apparently corresponds to the buried margin of a sunken central basin that existed in the caldera during the 19th century, as described and mapped by Macdonald (*3*). Point *A* in Fig. 10 (right) has the highest apparent temperature of the thermal anomalies associated with Kilauea. It is the vent and spatter cone of the July 1961 eruption into the floor of Halemaumau, and it is located where the southwest rift zone intersects the crater wall. Rock temperatures of 100°C are measured here about a meter below the surface (see *8*).

At Kilauea Iki, an intense thermal anomaly was recorded at the apex of the cinder cone (*B* in Fig. 11) on the southwest flank of the crater, immediately adjacent to the vent. Cinders on the crest of the cone are a bright yellow, in contrast to dull gray on the flanks and base. This color contrast, evident in the tones on the conventional photograph (Fig. 8), is attributed to pneumatolytic alteration and deposition. The lava lake, formed during the 1959–60 eruption, is about 110 meters deep; the solidified crust is now about 15 meters thick (*9*). The molten lava at the base of the crust has a temperature of about 1065°C (*2*). A double row of vents (Fig. 11) bordering the lava lake and along the walls of Kilauea Iki runs near or along the peripheral fracture zone developed during back-drainage of the lava. It is evident that there are differences in the apparent surface temperature of the lava lake (Fig. 11, areas 1 and 2), though there are no known corresponding compositional differences. Moreover, there is nothing obvious in the lake-bottom configuration to account for the apparent variation in surface temperature. There are differences in the surface texture of the lava (Fig. 12), however, which relate to differences in cooling history. One anomaly adjacent to the caldera (*B* in Fig. 10, left) is surrounded by a broad area of diffuse brightness (marked with arrows). This broad area does not appear on other images. Its margins do not correspond to topographic or vegetation boundaries.

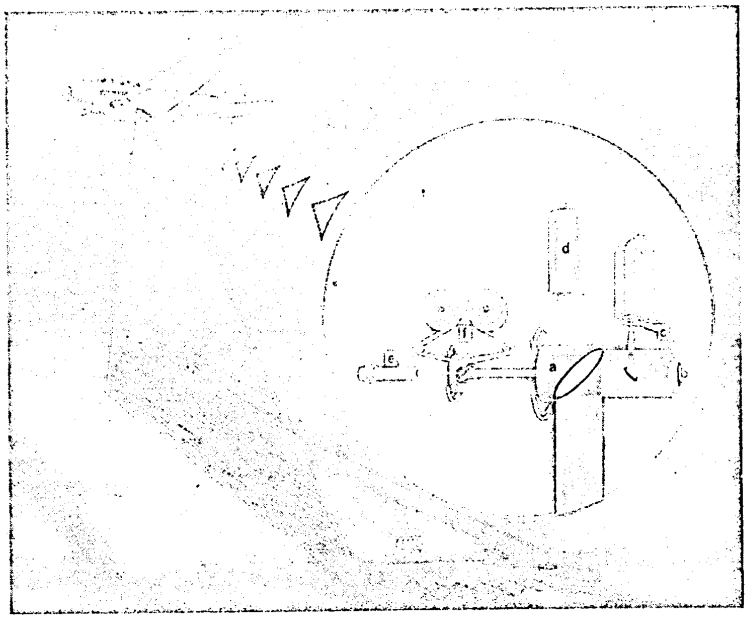

Fig. 4. Infrared scanning system. Radiation from the earth is collected on the surface of a rotating mirror *a*, reflected to the surface of a parabolic mirror *b*, and thence to the surface of a solid state detector *c*. The output of the detector is amplified *d* and modulates the output of a light source *e*. The modulated light is recorded on film *f*. Lateral coverage is obtained by rotation of the collecting mirror *a*; forward coverage is provided by forward movement of the aircraft and is coordinated with the recording film-transport mechanism. [Modified from diagram supplied by the H. R. B. Singer Corporation]

Southwest Rift Zone

The most recent eruption along the southwest rift zone took place in 1920 in an area about halfway between the summit and the sea. A few local thermal anomalies, not manifested on conventional aerial photographs (Figs. 8 and 13), were recorded along the rift zone approximately 3 kilometers southwest of Halemaumau (Fig. 14). Field investigations at one of these disclosed a series of small vents (Fig. 15) from which water vapor, at a temperature of 91°C, issues at velocities of 16 to 32 kilometers per hour. No color changes in the rock or other manifestations of thermal alteration were found, except for slight coloration immediately adjacent to the vents. No other thermal anomalies were found between those shown in Fig. 14 and the coast. At the intersection of the southwest rift zone with the coastline, however, a warm spring of significant size issues into the relatively cool ocean waters.

Chain of Craters and East Rift Zone

The thermal expression of some volcanic features along the Chain of Craters (Fig. 16, top and bottom) in the summit area of the east rift zone appears differently on the two images, owing to differences in electronic gain, photographic processing, and time of recording. Some differences may also relate to changes in apparent temperature.

The linear thermal source *B* of Fig. 16 is faintly visible on images for the 2.0- to 2.6-μ region of the spectrum, and thus its temperature was significantly higher than ambient temperature on 17 February. It is likely that the linearity of this source relates to

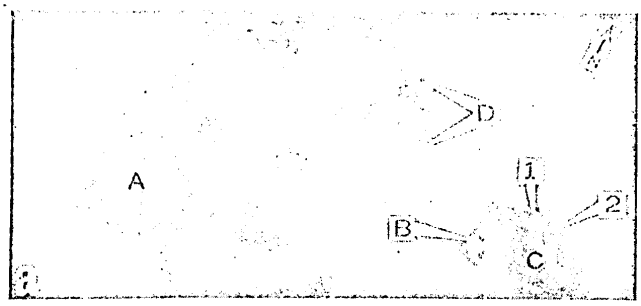

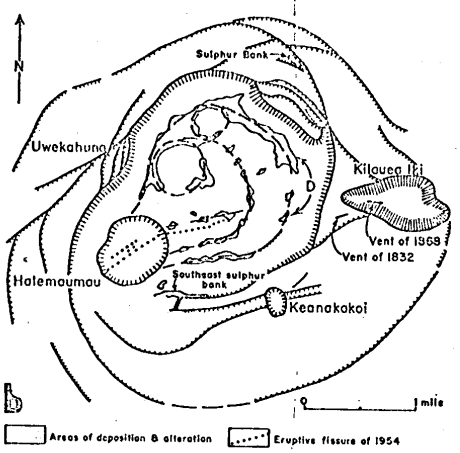

Fig. 11. (*a*) Infrared image of Kilauea summit area. Time, 0702, 28 January; spectral region, 4.5 to 5.5 μ; altitude, 1800 meters. *A*, Halemaumau; *B*, cinder cone formed during eruption of 1959; *C*, Kilauea Iki areas 1 and 2 shown in Fig. 12. (*b*) Map of Kilauea caldera, showing areas of pneumatolytic deposition and alteration. *D*, Suspected margin of inner basin in 1840. [From Macdonald (*3*)]

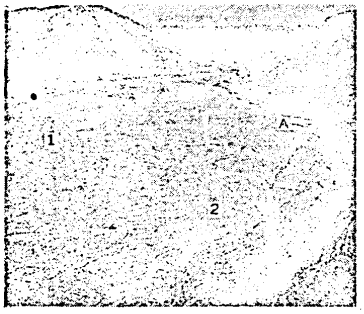

Fig. 12 (above). The floor of Kilauea Iki, as one looks westward. 1 and 2, Parts of the floor having different surface configurations. The line of contact between areas 1 and 2 is indicated by arrows. *A*, Peripheral fractures at the edge of congealed lava.

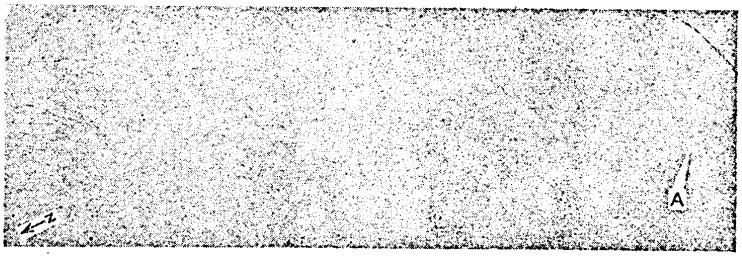

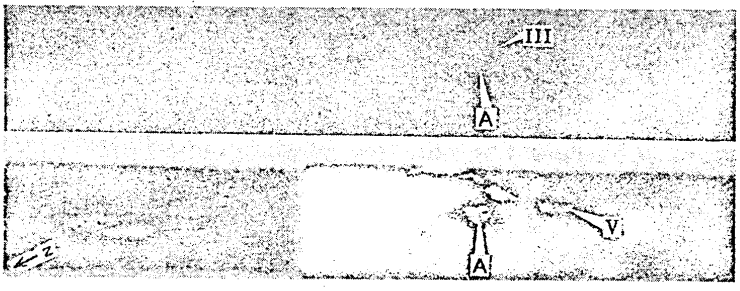

Fig. 13 (top, right). Conventional aerial photograph of area shown in Fig. 14. *A*, Area shown in Figs. 14 and 15.

Fig. 14 (middle, right). Infrared image of part of the southwest rift zone. Time, 0610, 17 February; altitude, 900 meters; spectral regions: top image, 2 to 2.6 μ; bottom image, 1.9 to 5.5 μ. *A*, Area shown in Figs. 13 and 15. On bottom image, note the progressive decrease in temperature with increase in ground elevation along the flight path, requiring a change in electronic gain. Roman numerals indicate orders of magnitude of apparent temperature.

Fig. 15 (bottom, right). Ground photograph of a steaming vent associated with thermal source *A* in Figs. 13 and 14. *A* in this figure indicates a cigarette, included for scale.

a similarly aligned fracture which forms the northwest margin of the anomaly and which may form a path for hot gases escaping from below.

The low apparent temperatures of the floor of Keanakakoi and some other craters along the rift zone are believed to be caused by deposits of cinders on the crater floors. Repetitive observations of cinders discharged during the 1959–60 eruption suggest that, in early morning hours, cinders emit less energy than other surficial materials do.

The most thermally active area along the Chain of Craters is at Aloi, the site of the 7 December 1962 eruption. A lava lake 13½ meters thick was formed at that time, but subsequent drainback reduced its depth to 4½ meters (*10*). Copious amounts of steam issue from fractures in and surrounding the crater. Surface cracks associated with these fractures were observed to both lengthen and increase in breadth during the course of the investigations. Field temperature measurements of a small thermal source near one of the steaming surface cracks (*A* in Fig. 16, bottom) varied from day to day but, on the whole, increased from 37°C (28 January) to 46°C (17 February). On the infrared images Aloi Crater shows a slightly off-center vent and a peripheral ring. The large hot area, southwest of the crater, is a steaming area that lies along a northeast-trending fault system.

Linear thermal sources extending eastward from Aloi and Alae craters (Fig. 17) are fractures associated with movement along the east rift and with lava from the December 1962 eruption. These linear thermal sources consistently display right offset, *en échelon* displacement, and a fishtailing or splaying of their eastern termini. Common-

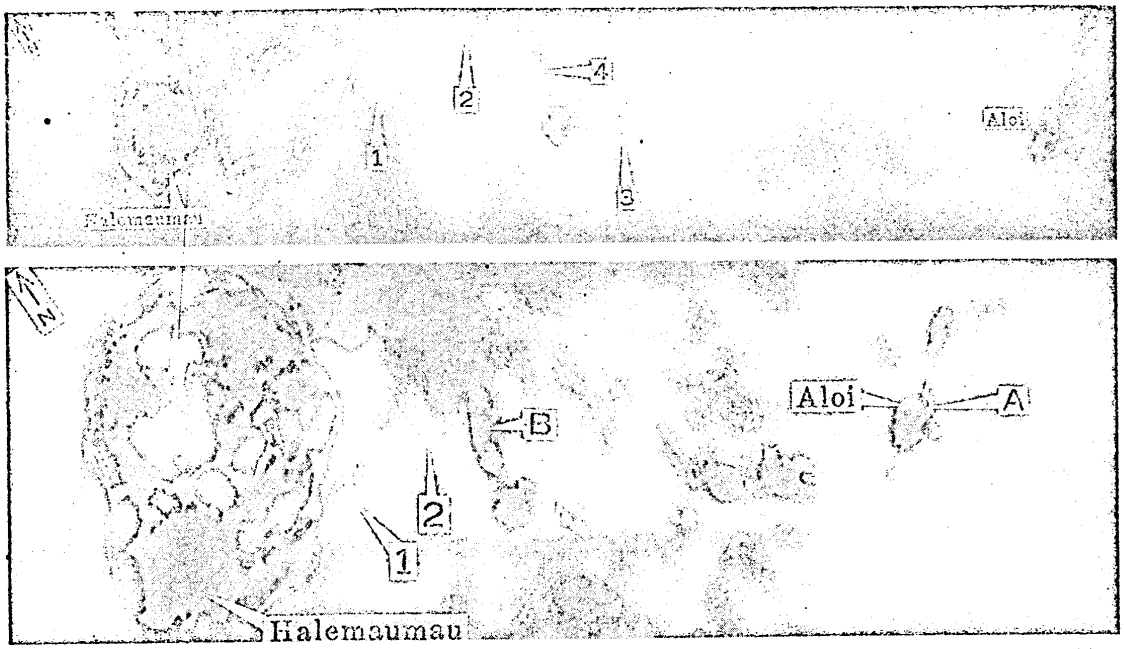

Fig. 16. Infrared images of Kilauea summit area and Chain of Craters. (Top) Time, 0800, 26 January; spectral region, 4.5 to 5.5 μ; altitude, 1800 meters. 1, Keanakakoi; 2, Lua Manu; 3, Kokoolau; 4, Puhimau. (Bottom) Time, 0455, 17 February; spectral region, 1.9 to 5.5 μ; altitude, 5100 meters. 1, Keanakakoi; 2, Lua Manu; *A*, thermal source near Aloi crater; *B*, linear thermal source. The bright linear streak passing through numeral 1 results from electronic malfunction.

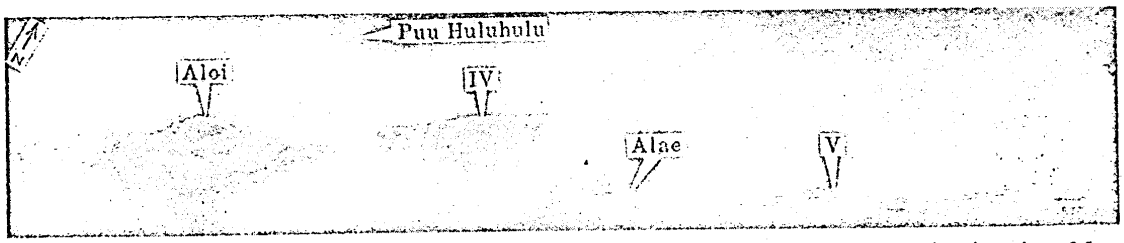

Fig. 17. Infrared image of part of the rift zone extending east from Aloi. Time, 0348, 14 February; spectral region, about 0.5 to 5.5 μ; altitude, 900 meters. Roman numerals indicate orders of magnitude of apparent temperature.

ly, the northern margins of the thermal sources are sharply defined; the southern margins are diffuse and irregular. In Fig. 17, wind streaming contributes to the diffuse south limits of the fracture patterns.

The thermal patterns of parts of the rift zone east of Aloi may have changed during the course of the investigations. Figures 18*a* and 18*b* are images of Alae Crater; there is an obvious difference in electronic gain on the two images, but, in addition, thermal sources appear in Fig. 18*b* that do not appear in 18*a*. Images produced at times between those of Fig. 18 suggest a progressive development of these features. An eruption occurred in, and adjacent to, Alae Crater on 22 August 1963, along a northeast-trending fracture (*10*) which passes through the thermal sources shown in Fig. 18*b*. Figure 19 shows images of Napau Crater, approximately 5 kilometers east of Alae. An eruption occurred along this lineament on 6 October 1963 (*10*). Images of Napau Crater were recorded 12 times from 26 January to 20 February. The thermal anomaly, indicated by the unlabeled arrow in Fig. 19*b*, was first seen on 8 February on an image for the 8- to 14-μ region of the spectrum. As the survey progressed, the anomaly was detected at increasingly shorter wavelengths. Electronic gain settings varied from image to image, as shown in Figs. 19*a* and 19*b*; likewise, visible steaming associated with thermal anomalies is known to vary from time to time, and it is possible that this apparent change in thermal pattern relates entirely to one or both of these variables. The progressive development of this feature, however, and its appearance at successively shorter wavelengths, tempts us to speculate that its growth represents a change in the convective heat-transfer system associated with the ingress of magma prior to eruption.

Eastward from Napau Crater to the site of the former village of Kapoho (Fig. 3), the rift zone is expressed on infrared imagery by a series of warm *en échelon* fractures interspersed with thermal sources having roughly circular configurations. Additional apparent changes in thermal pattern were observed in this segment of the rift zone. One such change in an 8-day period occurs in an area approximately 16 kilometers east of Napau Crater (Fig. 20) along the north side of the rift zone in the September 1961 eruption area (*11*).

Figure 21 is a conventional aerial photograph showing the lava flow that destroyed the village of Kapoho. The initial events have been described by Richter and Eaton (*5*). "On 13 January strong earthquakes centered near the village of Kapoho, 28 miles east of Kilauea's summit, and an old graben (an elongated block which has subsided between a pair of normal faults) two miles long and half a mile wide, which contained part of the village and most of the farmland that sustained it, began to subside. By nightfall displacements along the faults bounding the graben had grown to several feet. . . . At 7:30 PM the flank eruption began along a line of *en échelon* fissures 0.7 of a mile long, a few hundred yards north of the village. . . . The main fountain area, two miles from the sea coast . . . soon produced a steady stream of lava that slowly flowed down through the graben, reaching the sea. . . ."

By the end of the week the graben had been filled, and lava then spread laterally over the adjacent land surface. The infrared image (Fig. 22) shows that the peripheral part of the flow has reached ambient temperatures, in marked contrast to the vent area at the western end and to the central, thicker part of the flow, which occupies the graben. Temperatures at the surface of a series of small vents, near

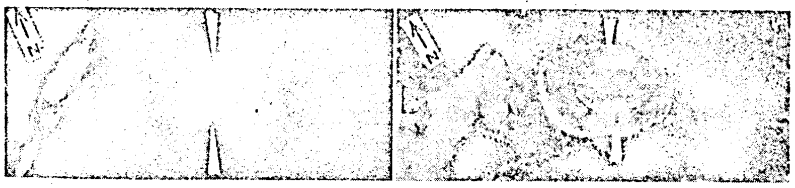

Fig. 18. Infrared images of Alae crater. (*a*) Time, 0710, 26 January; spectral region, 4.5 to 5.5 μ; altitude, 1800 meters. (*b*) Time, 0712, 20 February; spectral region, 4.5 to 5.5 μ; altitude, 900 meters. Arrows designate thermal sources visible on image *b* that do not appear on image *a*.

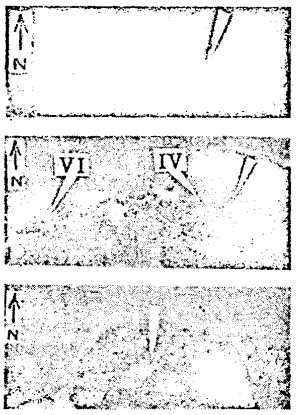

Fig. 19 (left). Infrared images of Napau crater. (*a*) Time, 1657, 1 February; spectral region, 4.2 to 5.5 μ; altitude, 600 meters. (*b*) Time, 0249, 14 February; spectral region, about 0.5 to 5.5 μ; altitude 900 meters. (*c*) Time, 0642, 20 February; spectral region, 4.5 to 5.5 μ; altitude, 360 meters. White arrows designate a thermal source that does not appear on image *a* but is visible on images *b* and *c*. Roman numerals indicate orders of magnitude of apparent temperature.

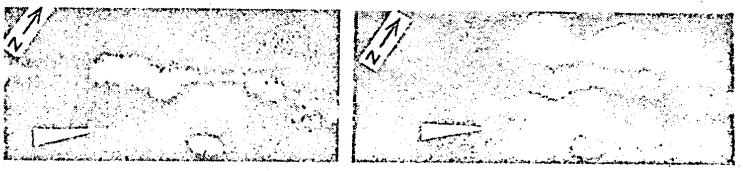

Fig. 20 (left). Infrared images of a part of the east rift zone east of Napau. (*a*) Time, 1800, 12 February; spectral region, about 0.5 to 5.5 μ; altitude, 750 meters. (*b*) Time, 0642, 20 February; spectral region, 4.5 to 5.5 μ; altitude, 750 meters. White arrows designate thermal source visible on image *b* which does not appear on image *a*.

the former site of the village of Kapoho, ranged from 26° to 108°C. Near the center of the Kapoho flow, rocks immediately below the surface have temperatures much higher than the 108°C measured at the surface. A contact pyrometer lowered about half a meter into a small fracture went off scale at 333°C.

Infrared Surveys of Other Hawaiian Volcanoes

During the course of the investigation, one or more flights were made over the rift zones associated with Mauna Loa, Hualalai, and Kohala volcanoes on the island of Hawaii (*7, 12*). Mauna Loa last erupted in 1950, Hualalai in 1801; Kohala has not been active in historic time. To facilitate navigation, these flights were made shortly after dawn. No thermal activity was observed on Kohala or Hualalai; some thermal sources, however, were evident on the southwest rift zone of Mauna Loa, and warm springs flowed into the sea near where the rift

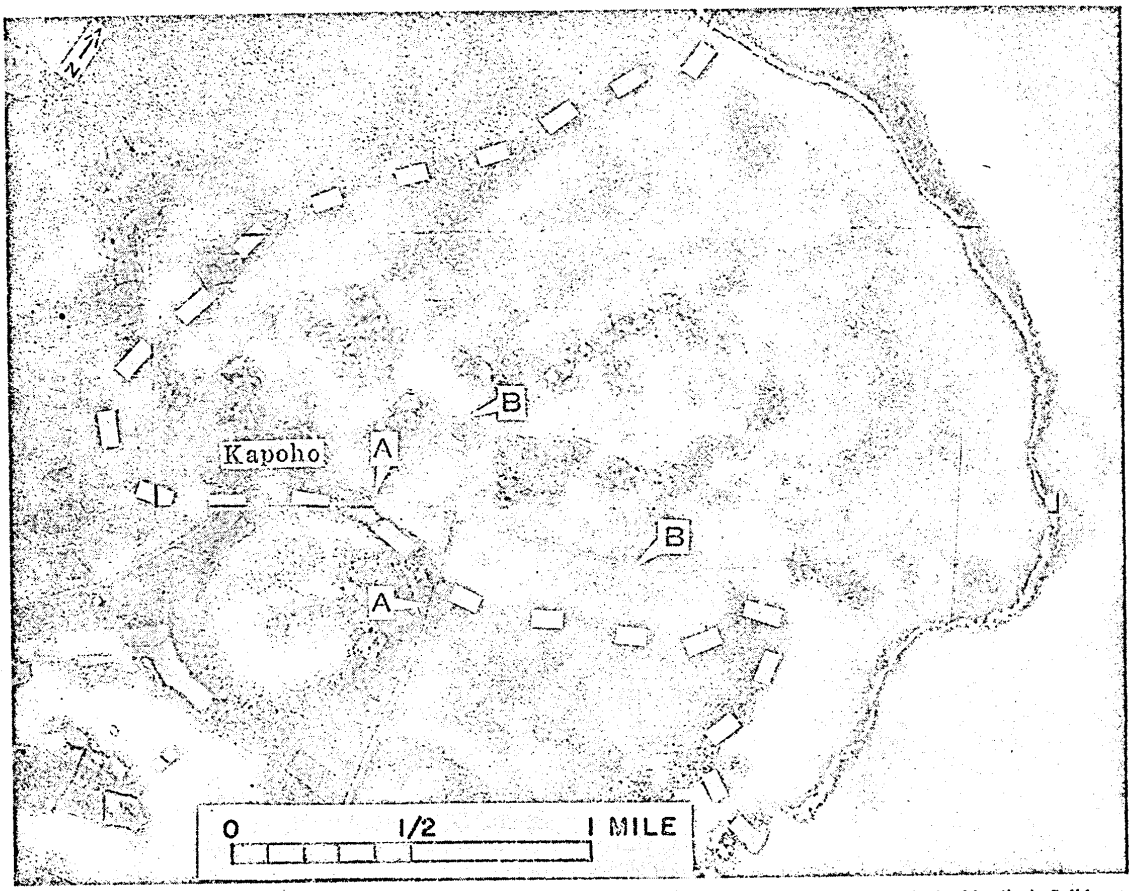

Fig. 21. Conventional aerial photograph of the Kapoho area showing areal extent of 1960 lava flow (dashed white line). Solid outline indicates the area common to Figs. 21 and 22. *A* and *B* are the roads referred to in text, shown in Fig. 25.

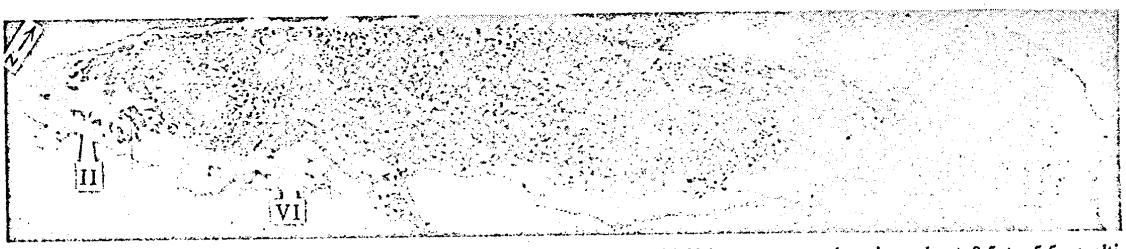

Fig. 22. Infrared image of a part of the Kapoho flow of 1960. Time, 0340, 14 February; spectral region, about 0.5 to 5.5 μ; altitude, 900 meters. Flow originated near vent at west end.

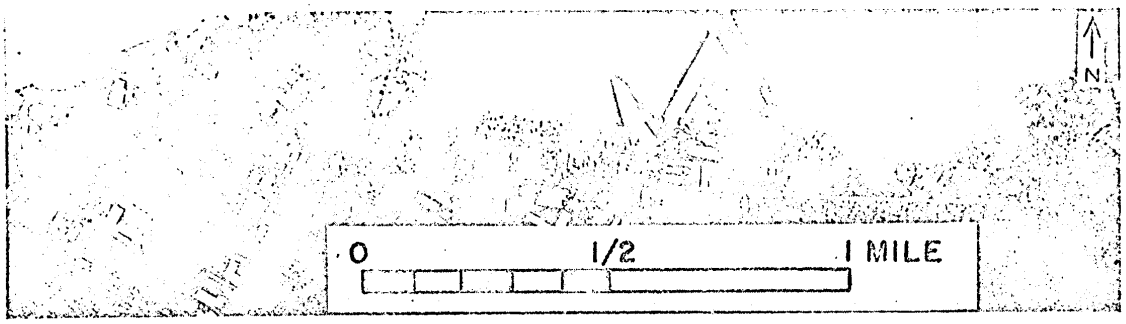

Fig. 23. Conventional aerial photograph of the coastline east of Hilo.

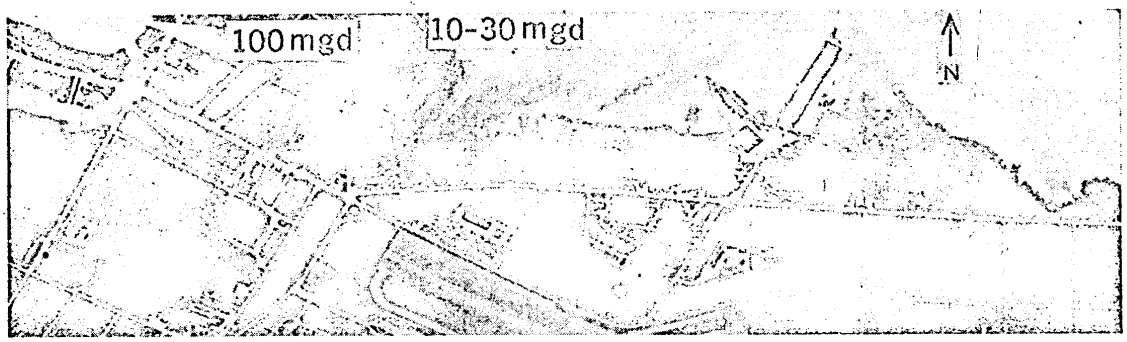

Fig. 24. Infrared image of the part of the coastline shown in Fig. 23. Time, 0723, 19 February; spectral region, 4.5 to 5.5 μ; altitude, 900 meters. Dark areas in the ocean area are believed to represent cool water discharged by springs. Numerals are estimated rates of flow of springs in millions of gallons per day.

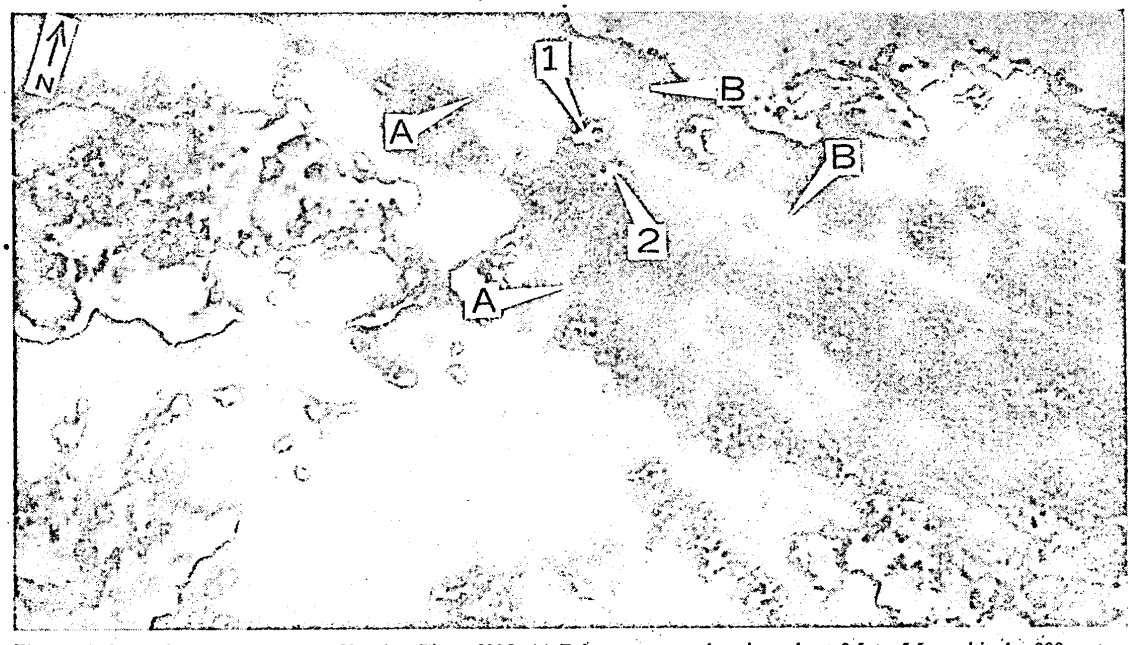

Fig. 25. Infrared image of area near Kapoho. Time, 0225, 14 February; spectral region, about 0.5 to 5.5 μ; altitude, 900 meters. *A*, Blacktop roads; *B*, roads surfaced with cinders. *1* and *2*, Thermal sources that extend beneath the blacktop roads. This area is also shown in Fig. 21.

zone intersects the coast. A single flight was made across the southern flank of Haleakala volcano on the island of Maui (*7*), which last erupted in 1750. Images produced on this flight, made in mid-afternoon, show no evidence of thermal activity.

Thermal Patterns in Water

There are few well-developed streams on the island of Hawaii, as most rain water percolates downward through the highly permeable volcanic rocks. Because it is less dense than the saline ocean waters, the fresh water "floats" outward and is discharged into the ocean. The ground water commonly has a lower temperature (measurements in caves suggest a temperature of about 15°C) than the ocean (about 20°C).

Because the emissivity of water is essentially uniform and near unity, changes in film density on the infrared images almost certainly relate to changes of the surface temperature of the water, provided the sky temperature is uniform. Thus, large discharges of fresh ground water can be recognized from their thermal contrast with the ocean and from the pattern of discharge. More than 25 major spring areas on the periphery of the island of Hawaii are visible on the infrared images (*13*). Most of these springs have low apparent temperature in contrast to that of the sea water; some, however, adjacent to the northeast and southwest rift zones of Kilauea, have relatively high apparent temperatures.

An infrared image of the coastline east of Hilo shows the cooler (darker) water impounded by a breakwater (Figs. 23 and 24). Darker, northeast-trending streaks are also evident. Their orientation and shape and the fact that they are cooler than the ocean suggest springs discharging large quantities of fresh ground water into the ocean. The flow rates estimated from ground observation (*14*) are given in Fig. 24.

Engineering Geologic Information

Cinders are widely used as a construction material on the island of Hawaii. They can commonly be recognized on infrared images by high apparent temperatures in daylight hours and relatively low apparent temperatures in early morning hours (as at the floor of Keanakakoi, Fig. 16). This characteristic is further illustrated in Figs. 21 and 25. The blacktop roads (*A* in Fig. 21) and roads surfaced with cinders (*B* in Fig. 21) absorb similar amounts of visible solar energy. The infrared image (Fig. 25), however, shows that more radiation is emitted from the roads surfaced with cinders.

Numerals 1 and 2 in Fig. 25 designate thermal sources which extend beneath the blacktop roads and which consequently may have a detrimental long-range effect on the road surface.

The foregoing relationship between absorption of solar energy and emission of infrared energy suggests that these parameters may provide clues to the configuration and physical composition of surficial materials, and that they may be particularly useful where surfaces cannot be adequately resolved on conventional photographs.

Summary

Aerial infrared-sensor surveys of Kilauea volcano have depicted the areal extent and the relative intensity of abnormal thermal features in the caldera area of the volcano and along its associated rift zones. Many of these anomalies show correlation with visible steaming and reflect convective transfer of heat to the surface from subterranean sources. Structural details of the volcano, some not evident from surface observation, are also delineated by their thermal abnormalities. Several changes were observed in the patterns of infrared emission during the period of study; two such changes show correlation in location with subsequent eruptions, but the cause-and-effect relationship is uncertain.

Thermal anomalies were also observed on the southwest flank of Mauna Loa; images of other volcanoes on the island of Hawaii, and of Haleakala on the island of Maui, revealed no thermal abnormalities.

Approximately 25 large springs issuing into the ocean around the periphery of Hawaii have been detected.

Infrared emission varies widely with surface texture and composition, suggesting that similar observations may have value for estimating surface conditions on the moon or planets.

References and Notes

1. T. A. Jagger, *Hawaiian Volcano Obs. Bull.* **7**, 77 (1922); **9**, 107 (1922); **10**, 113 (1922).
2. W. A. Ault, D. H. Richter, D. B. Stewart, *J. Geophys. Res.* **67**, 2809 (1962).
3. G. A. Macdonald, *Volcano Letter No. 528* (1955), p. 1.
4. *Aviation Week* **72**, No. 8, 76 (1960). For an excellent review of the state of the art as of 1959, see *Proc. I.R.E. (Inst. Radio Engrs.)* **47** (Sept. 1959).
5. D. H. Richter and J. P. Eaton, *New Scientist* **7**, 994 (1960).
6. H. T. Stearns and G. A. Macdonald, *Hawaii Div. Hydrography Bull. 9* (1946); G. A. Macdonald and J. P. Eaton, *U.S. Geol. Surv. Bull. 1171* (1964), p. 1.
7. H. T. Stearns, *Hawaii Div. Hydrography Bull. 8* (1946).
8. J. B. Moore, written communication, Feb. 1964.
9. H. Krivoy, written communication, Oct. 1963.
10. J. G. Moore, written communication, Oct. 1963.
11. ——— and D. H. Richter, *Geol. Soc. Am. Bull.* **73**, 1153 (1962).
12. G. A. Macdonald and D. H. Hubbard, *Volcanoes of the National Parks in Hawaii* (Hawaii Natural History Association, 1961).
13. W. A. Fischer, R. M. Moxham, T. M. Sousa, D. A. Davis, "U.S. Geol. Surv. Misc. Geol. Invest. Map," in preparation.
14. D. A. Davis, written communication, Mar. 1963.
15. Publication of this article is authorized by the director of the U.S. Geological Survey. We gratefully acknowledge the assistance given by James G. Moore, Scientist-in-Charge, Hawaiian Volcano Observatory, and his staff. Dr. Moore provided assistance in the field and continues to supply many relevant observations. Howard A. Powers pointed out several of the geologic features related to the thermal patterns. We also thank Commander D. W. Linker, U.S. Navy, for assistance in the field and for his personal interest and initiative, which did much to facilitate this investigation; Jack C. Pales and the staff of the Mauna Loa Observatory, U.S. Weather Bureau, for guidance and for the use of darkroom facilities; Robert Beals for reconnaissance flights; Major Paul K. Nakamura, Hawaiian National Guard, for providing hangar facilities; and the U.S. Army Electronics Command for making available an infrared scanning system. Alva B. Clarke provided valuable assistance in photographic and image processing.